Engineering and Technology Journal
Journal homepage: https://etj.uotechnology.edu.iq

A combining two ksvm classifiers based on True pixel values and Discrete wavelet transform for mri-based brain tumor detection and Classification

Ali A. Mohammed*, Mohammed A. Noaman , Hassan M. Azzawi

Electrical Engineering Dept., University of Technology-Iraq, Alsina'a street, 10066 Baghdad, Iraq.
*Corresponding author Email: eee.19.28@grad.uotechnology.edu.iq

HIGHLIGHTS

- We have proposed an integrated algorithm to classify brain tumors following two stages.
- We have used the Kernel Support Vector Machine (KSVM) classifier.
- The linear kernel achieved 97.5% accuracy and 98.57% accuracy in the first and second classifiers.

ARTICLE INFO

Handling editor: Ivan I. Hashim

Keywords:
MRI
SVM
DWT
PCA

ABSTRACT

The studies on brain tumor detection and classification are continuing to improve the specialists' ability in diagnosis. Magnetic Resonance Imaging (MRI) is one of the most common techniques used to evaluate brain tumors diagnosis. However, brain tumors diagnosis is a difficult process due to congenital malformations and possible errors in diagnosing benign from malignant tumors. Therefore, this research aims to propose an integrated algorithm to classify brain tumors following two stages using the Kernel Support Vector Machine (KSVM) classifier. First stage classifies the tumors as normal and abnormal, and the second classifies abnormal tumors as benign and malignant. The first KSVM employs extraction features by considering the pixel values to classify images as a shape. In contrast, the second KSVM uses the Discrete Wavelet Transform (DWT), followed by the Principal Component Analysis (PCA) technique to extract and reduce features and improve the model performance. Also, K-means clustering algorithm is used to segment, isolate and calculate the tumor area. The KSVM classifiers use two kernels (linear and Radial Basis Function (RBF)). Obtained results showed that the linear kernel achieved 97.5% accuracy and 98.57% accuracy in the first and second classifier, respectively. For all linear classifiers, a 100% sensitivity level is achieved. This work validates the proposed model based on the (K-fold) strategy.

1. Introduction

Brain tumor is a complicated health problem determined by many cancer research centers around the world. In 2016, World Health Organization (WHO) encourage neurooncological specialists worldwide to develop a verified classification system for brain tumor diagnosis. [1]. Therefore, different neurooncological techniques are adapted to help a valid detection and classification for brain tumor diagnosis. One of the most common methods is a Magnetic Resonance Imaging (MRI) scan [2]. MRI provides essential information about brain anatomy, which helps the specialist with important tumor information [2]. Analysing medical images is schemed through several stages to optimize brain tumour detection and classification as well as reduce error ratios. Pre-processes image is the earlier stage in the whole process, in which different extents of imagery noises could be observed or take place and therefore reduce appropriate contrast [2, 3]. MRI images frequently include undesirable parts that may reduce image visualization. Therefore, de-noising process for the medical images is critical to improve visual quality and help to better disease diagnosis. De-noising is achieved by using different filter types such as Median filter, Gaussian filter, and Adaptive filter [3, 4]. The performance of the noise removal algorithm can be evaluated using several parameters such as Peak Signal to Noise Ratio (PSNR), Mean Square Error (MSE), and Root Mean Square Error (RMSE) [4]. Literatures context about medical image visualization are varied based on the purpose; aim and objectives. However, Brain tumour classification occupies many studies to decide the infected brain, which substantial for any research interested in class classification. For this purpose, several classifiers can be used, such as Kernel Support Vector Machine (KSVM) [3, 5]. The KSVM classifier is an efficient technique that provides an accurate forecast and classification. The KSVM classifier can classify images into normal and abnormal [5, 6] or benign and malignant tumours [7,8] It requires specific training of the extracted features which are necessary for any image-based applications [9]. The feature extraction can be achieved by a Discrete Wavelet Transform (DWT)

http://doi.org/10.30684/etj.v40i2.2180
Received 24 May 2021; Accepted 14 June 2021; Available online 25 February 2022
2412-0758/University of Technology-Iraq, Baghdad, Iraq

[10] or by the shape analysis method to retrieve and recognize the objects represented in the images [11]. In addition, the abnormal cases can be segmented by clustering techniques [12] such as K-means, which is the simplest unsupervised machine learning algorithm [7]. This method supports the isolating and calculation of the tumour area.

To evaluate a proposed machine learning model, cross-validation is a substantial method that can estimate the performance of the designed model. Several techniques are used for assessing, such as K-fold cross-validation [13, 14] which is an efficient and simple method. This paper aims to improve the precision of MRI brain tumor classification and help the specialist make an accurate decision. Thus, it makes the following contributions:

1) Proposes an integrated algorithm by combining two KSVM classifiers to detect normal and abnormal brains, benign and malignant tumors.
2) Develop a simple method of feature extraction to classify normal and abnormal brains.
3) Perform K-fold cross-validation to estimate the proposed algorithm

The rest of this paper is organized as follows: Section 2: presents a complete explanation of the proposed algorithm. Section 3: explains the K-fold cross-validation method used to evaluate the proposed model. Section 4: demonstrates the results and the evaluation metrics of the proposed model. Section 5: Makes cross-validation of our classifiers based on the K-fold technique. Section 6: discusses the paper's results in comparison with previous studies. And Section 7: concludes the entire work.

2. Proposed method

The work of this paper uses the data that has been collected by The Cancer Imaging Archive (TCIA) and Cagle [15, 16] our proposed method designs an integrated algorithm to classify MRI images and detect brains tumour. It isolates and finds brain tumour boundaries, and calculates the tumour area. In addition, the method classifies tumours as malignant or benign. Figure 1 illustrates the flowchart of the entire proposed method. This section describes the accurate and obvious steps of the methodology that has been used in this work.

2.1 Pre-processing

The initial stage in our proposed method is the MRI image pre-processing. This stage converts images into a cleared format by removing and minimizing noise using linear spatial filtering[17]. In this step, we do not focus on the different types of noise filtering techniques. The calculation of the output (g(x, y)) of the linear spatial filtering of an image of size $m \times n$ with a filter of size $M \times N$ can be expressed as in Eq. (1).

$$g(x,y) = \sum_{s=-a}^{a} \sum_{t=-b}^{b} w(s,t).f(x+s,y+t) \quad (1)$$

Where w is filter coefficients (mask), f is the image pixels values, $a = (M-1)/2$, and $b = (N-1)/2$. To generate a complete filtered image, the Eq. (1) must be applied for $x = 0, 1, 2\ldots, m-1$ and $y = 0, 1, 2\ldots., n-1$. X and y are varied then each pixel in w visits every pixel in f.

2.2 Support vector machine (SVM) classifier

The SVM classifier is one of the popular algorithms that can perform well in classification methods. It is a linear classifier that works in a simple strategy to find an optimal hyper plane with a maximum margin differentiating the classes. However, the support vectors, or feature vectors, might not be linearly separable. In this case, the SVM introduces the kernel function, such as linear function, polynomial, and radial basis function (RPF) [18, 19].

The linear kernel function $K(x, x_i)$ of the vectors, x and x_i are usually described as in Eq. (2).

$$K(x,x_i) = x.x^T \quad (2)$$

Figure 2 shows a graphical representation of the linear kernel function.

The RBF kernel function $K(x, x_i)$ depends on its calculation of the distance from some point. It describes as in Eq. (3).

$$K(x,x_i) = e^{-\gamma \|x-x_i\|^2} \quad (3)$$

Where $||x - x_i||$ is Euclidean distance between x & x_i, and kernel function parameter $\gamma > 0$.

Figure 3 shows a graphical representation of the RBF kernel function. In this work, the classifier is used two times to classify the brain as normal and abnormal initially, and subsequently classify the brain tumor as benign and malignant. As shown in Figure 1, the classifiers in the proposed algorithm are denoted as KSVM-1 and KSVM-2. The evaluation metrics (accuracy, sensitivity, and specificity) can assess the results achieved by the KSVM [5, 20]. They are the probability measures for classification precision. Accuracy is a measure for the dataset categorization, sensitivity is a measure for the abnormal cases anticipated, and specificity is a measure for normal cases expected. Table 1 explains the calculations of evaluation metrics.

The confusion matrix, also known as the error matrix, defines the terms from the actual results (ground truth) and the expected results of evaluation metrics calculations, as shown in Table 2. The terms of actual results are (True Positive (TP), True Negative (TN), False Positive (FP), and False Negative (FN)). TP means correctly diagnosed as diseased, TN means correctly diagnosed as not diseased, FP means incorrectly diagnosed as diseased, and FN means incorrectly diagnosed as not diseased).

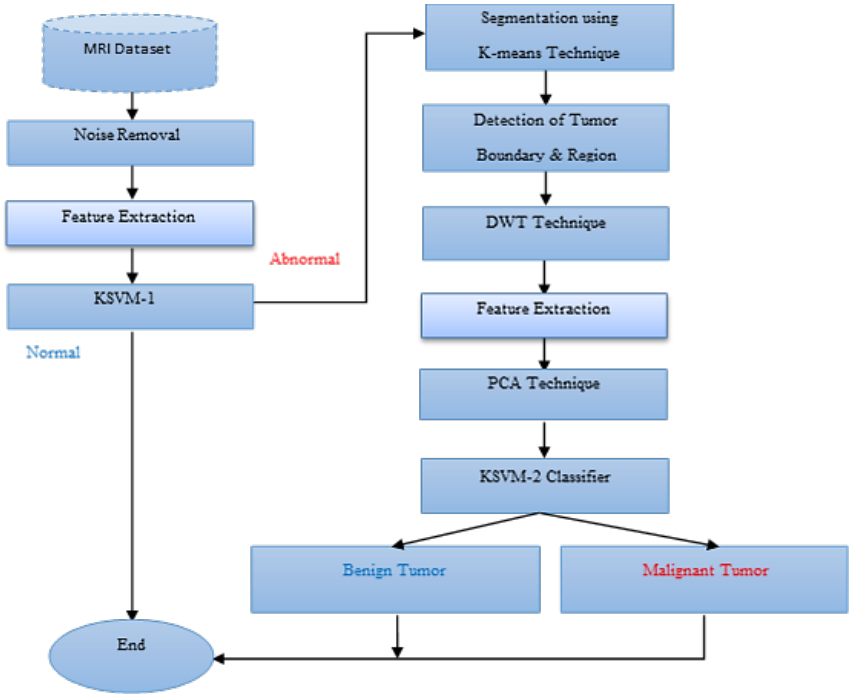

Figure 1: Flow chart of the proposed system

2.3 K-means clustering

The clustering process can confirm the process of targeting the affected area. The brain is segmented using the K-means clustering algorithm, and the tumour area is isolated using the characteristic of the area [12]. We calculate the number of image pixels *NP* and the size of the tumor region as in Eq. (4).

$$NP = \sum_{n=0}^{255} \sum_{m=0}^{255} [f(0) + f(1)] \quad (4)$$

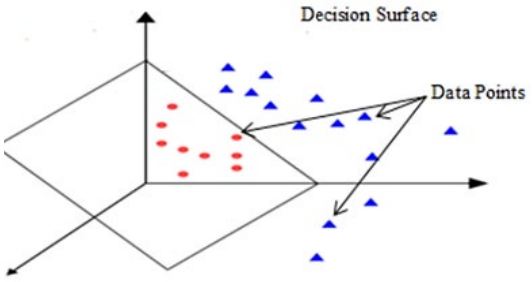

Figure 2: Linear kernel representation

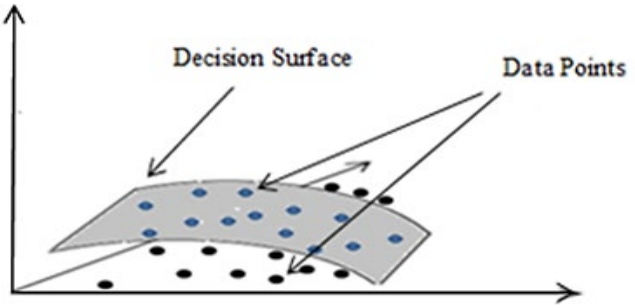

Figure 3: RBF kernel representation

Table 1: Calculations of evaluation metrics

Evaluation Metric	Equation
Accuracy	$\frac{TP + TN}{TP + TN + FP + FN}$
Sensitivity	$\frac{TP}{TP + FN}$
Specificity	$\frac{TN}{TN + FP}$

Table 2: Confusion matrix defining the terms TP, TN, FP, and FN

		Actual results		Row Total
		Negative	***Positive***	
Expected result	Positive	TP	FP	TP+FP
Expected result	Negative	FN	TN	FN+TN
	Column total	TP+FN	FP+TN	TP + FP + FN + TN

Where $f(0)$ is black pixels, and $f(1)$ is white pixels. One pixel equal to $0.264\ mm^2$. And the number of white pixels *WP* that is our target of the study is calculated as follows:

$$\mathrm{WP} = \sum_{n=0}^{255} \sum_{m=0}^{255} f(1) \tag{5}$$

Then we can calculate the tumour area A as follow:

$$\mathrm{A} = \sqrt{P} \times 0.264 \tag{6}$$

2.4 Discrete wavelet transform (dwt)

DWT is an effective numerical analysis method useful in MRI image classification, pathological and abnormal brain detection [21]. Usually, it is used to extract necessary global features to support the classification techniques [22]. The fundamentals of DWT can be explained mathematically as follows. Assume that x(t) is a square-integral function, then the Continuous Wavelet Transform (CWT) of x(t) to a given wavelet φ(t) is defined as follows [14]:

$$W_{\varphi}(a,b) = \int_{-\infty}^{\infty} x(t)\varphi_{a,b}(t)dt \tag{7}$$

Where the wavelet $\varphi_{a,b}(t)$ is obtained from the mother wavelet $\varphi(t)$ by translation and dilation and it is calculated as follows [14]:

$$W_{\varphi}(a,b) = \int_{-\infty}^{\infty} x(t)\varphi_{a,b}(t)dt \tag{8}$$

a and b are the dilation factor and the translation parameter respectively, and both are real positive numbers. One of the most familiar wavelets is the Harr wavelet, which is often the preferred wavelet in several applications. Eq. (8) can be discretized to give the DWT by restraining a, b to a discrete lattice (a = 2b and a > 0). Thus, DWT can be expressed as follows [14]:

$$ca_{j,k}(n) = DS\left[\sum_n x(n) g_j^*(n - 2^j k)\right] \tag{9}$$

$$cd_{j,k}(n) = DS\left[\sum_n x(n) h_j^*(n - 2^j k)\right] \tag{10}$$

Where $ca_{j,k}$ denotes for the coefficient of the approximation components, and $cd_{j,k}$ denotes for the coefficient of the detail components. $g(n)$ refers to a low-pass filter, and $h(n)$ refers to a high-pass filter. j refers to the wavelet scale, and k refers to the translation factor, and *DS* is the down sampling. The equations in (10) and (11) decompose the signal $x(n)$ into two signals, and this procedure is called one-level decompose [14, 21]. Figure 4 demonstrates the process of DWT. The Two-Dimensional (2-D) DWT for images is similar to the DWT case. The 2-D DWT applies to each diminution separately. It leads to a decomposition of ca_n, in four sub-band components as shown in Figure 5: the approximation at level ca_{j+1}, and details sub-bands (ch_{j+1} is horizontal sub-band, cv_{j+1} is vertical sub-band, and cd_{j+1} is diagonal sub-band), where j is scaling factor [23].

2.5 Features extraction

To improve the classification metrics, two methods are implemented to extract features. For KSVM-; we train the classifier based on the pixel values of the brain images in the size of (200 × 200) pixels. In other words, we use the pixel values as a feature that reflects the diversity in the shapes of the images. For KSVM-2, we use the popular methods, the first-order and second-order statistic tools. The first-order tools represent a gray-level distribution of image pixels regardless of their spatial arrangement calculate the features (Mean (M_e), Standard Deviation (SD), Skegness (S_K), Kurtosis (K_{urtk}), and Entropy (E)) [24]. In contrast, we use the second-order statistic tools, Gary level Co-occurrence Matrix (GLCM) [24], which simultaneously involves two pixels to calculate the features (Energy ($E_{n)}$, Correlation (C_{orr}), Contrast (C_{on}), Homogeneity (H_{omo})). For an $m \times n$ size image, and the function of image pixel value $f(x,y)$, the extracted features are calculated as explained in the section below.

2.5.1 Mean: for an image

the mean is calculated by adding all the pixel values divided by the total number of pixels.

$$M_e = \left(\frac{1}{m\times n}\right)\sum_{x=0}^{m-1}\sum_{y=0}^{n-1} f(x,y) \tag{11}$$

2.5.2 Standard deviation

The standard deviation is a measure of the amount of variation of the image pixels.

$$SD = \sqrt{\left(\frac{1}{m\times n}\right)\sum_{x=0}^{m-1}\sum_{y=0}^{n-1} (f(x,y) - M)^2} \tag{12}$$

2.5.3 Skewness

Skewness is a measure of symmetry. The Skewness of a random variable X is:

$$S_k(X) = \left(\frac{1}{m\times n}\right)\frac{\sum(f(x,y)-M)^3|}{SD^3} \tag{13}$$

2.5.4 Kurtosis

The Kurtosis is the parameter describing the shape of a random variable probability distribution. The Kurtosis of a random variable X is:

$$\mathrm{K_{urtk}(X)} = \left(\frac{1}{\mathrm{m\times n}}\right)\frac{\sum(\mathrm{f(x,y)-M})^4|}{\mathrm{SD^4}} \tag{14}$$

2.5.5 Entropy

Entropy is a scale to describe the randomness of the textural image.

$$\mathrm{E} = -\sum_{\mathrm{x=0}}^{\mathrm{m-1}}\sum_{\mathrm{y=0}}^{\mathrm{n-1}} \mathrm{f(x,y)}\log_2 \mathrm{f(x,y)} \tag{15}$$

2.5.6 Energy

Energy is a measure of the similarity of an image. It is the quantifiable amount of the extent of pixel pair recurrences.

$$\mathrm{E_n} = \sqrt{\sum_{\mathrm{x=0}}^{\mathrm{m-1}}\sum_{\mathrm{y=0}}^{\mathrm{n-1}} \mathrm{f^2(x,y)}} \tag{16}$$

2.5.7 Correlation

The correlation describes the spatial dependencies between the pixels.

$$\mathrm{C_{orr}} = \frac{\sum_{\mathrm{x=0}}^{\mathrm{m-1}}\sum_{\mathrm{y=0}}^{\mathrm{n-1}}\mathrm{(x,y)f(x,y)-M_xM_y}}{\sigma_\mathrm{x}\sigma_\mathrm{y}} \tag{17}$$

2.5.8 Contrast

Contrast is an intensity measure of a pixel and its neighbour over the image.

$$C_{on} = \sum_{x=0}^{m-1}\sum_{y=0}^{n-1}(x,y)^2 f(x,y) \tag{18}$$

2.5.9 Homogeneity

Scales the local variations in image texture. The absence of intraregional changes in the image is indicated by High values of homogeneity. Consequently, locally homogeneous distribution in the image textures.

$$\mathrm{H_{omo}} = \sum_{\mathrm{x=0}}^{\mathrm{m-1}}\sum_{\mathrm{y=0}}^{\mathrm{n-1}}\frac{\mathrm{f(x,y)}}{1+\mathrm{(x-y)^2}} \tag{19}$$

2.6 Principal component analysis (pca)

Extra features reduce the processing performance by increasing the time and memory space. Thus, to reduce the size of extracted features, PCA is used [25]. The PCA is an effective normalizing technique that uses linear transformations to manipulate the data from high to low dimensional space. This method can be specified by eigenvectors of the covariance matrix as follows:

1) Find the mean value of the specified dataset S.
2) Obtain a new matrix A by subtracting the mean value from S.
3) Calculate a covariance 'C' from 'A'.

If the data 1,…,*l*, $A_k \in R^N, \sum_{k=1}^{l} A_k = 0$, the covariance matrix is:

$$C = \frac{1}{l} \sum_{i=1}^{l} A_k A_i^T \quad (20)$$

1) Obtain the eigenvalues for the covariance matrixes where are [V1, V2… VN].
2) Calculate eigenvectors from the covariance matrixes 'C'.

Any vector *S* or $S - \bar{S}$ can be written as a linear combination of eigenvectors as:

$$S - \bar{S} = b_1 u_1 + b_2 u_2 \ldots\ldots\ldots + b_n u_n \quad (21)$$

Obtain the lower-dimensional dataset from the largest eigenvalues.

$$S - \bar{S} = \sum_{i=1}^{l} b_i u_i \ , l < N \quad (22)$$

3. K-fold cross-validation

Cross-validation is a process used to assess a machine learning model skill on a finite data sample. In general, it is expected to carry out data that are not used during the model training. Cross-validation does not increase the final classification accuracy; it does give reliability to the classifier and can be generalized to another independent dataset. K-fold cross-validation is simple to understand and popular method, which results in a more optimistic estimate of the skill than other techniques [13]. A schematic diagram of 5-fold cross-validation illustrates in Figure 6, and it is described as follows [14]:

1) Shuffles the dataset randomly and splits it into K numbers of approximately equal size groups (folds).
2) For each particular fold, takes the one-fold as the dataset and the remaining fold K – 1 as a training dataset.
3) Fit a model on the training dataset and evaluate it on the test dataset. As such, record the error.
4) Repeats the process K times as the test dataset and average the error rates to obtain a comprehensive model validation error.

$$Err = \frac{1}{K} \sum_{i=1}^{K} Err_i \quad (23)$$

Where *Err* is the error rate, and so we can calculate the percentage of accuracy.

$$Acc = 100 - Err \times 100 \quad (24)$$

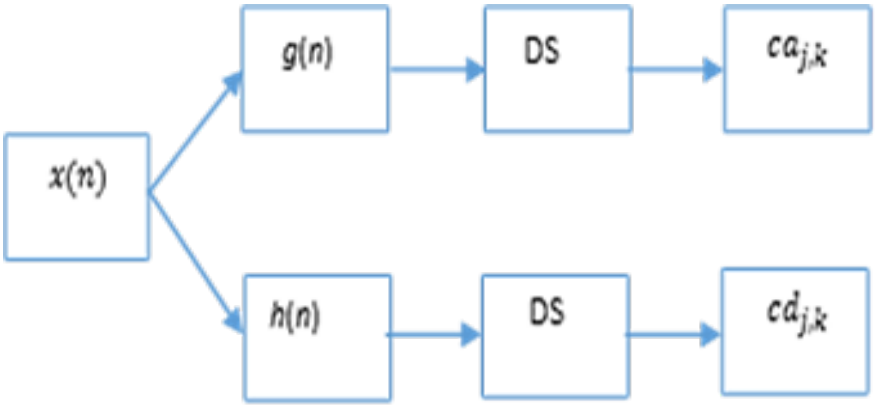

Figure 4: Schematic diagram of DWT

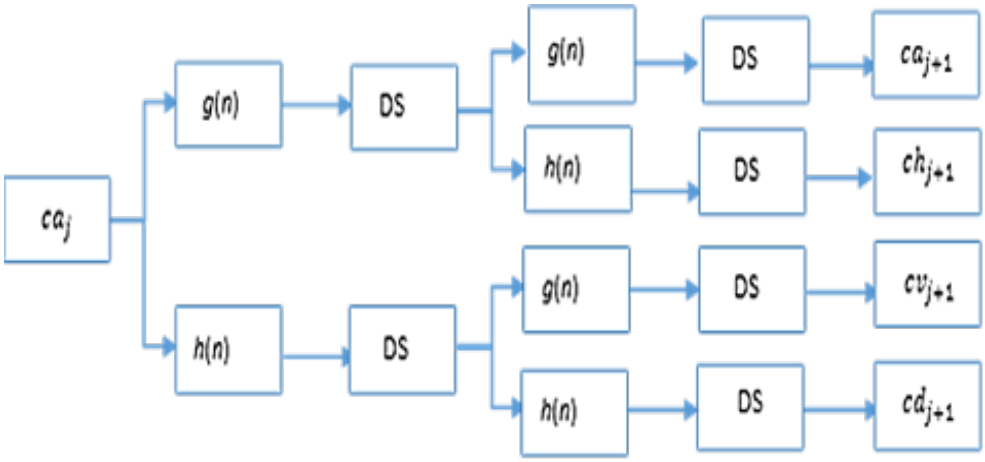

Figure 5: Schematic diagram of 2-D DWT

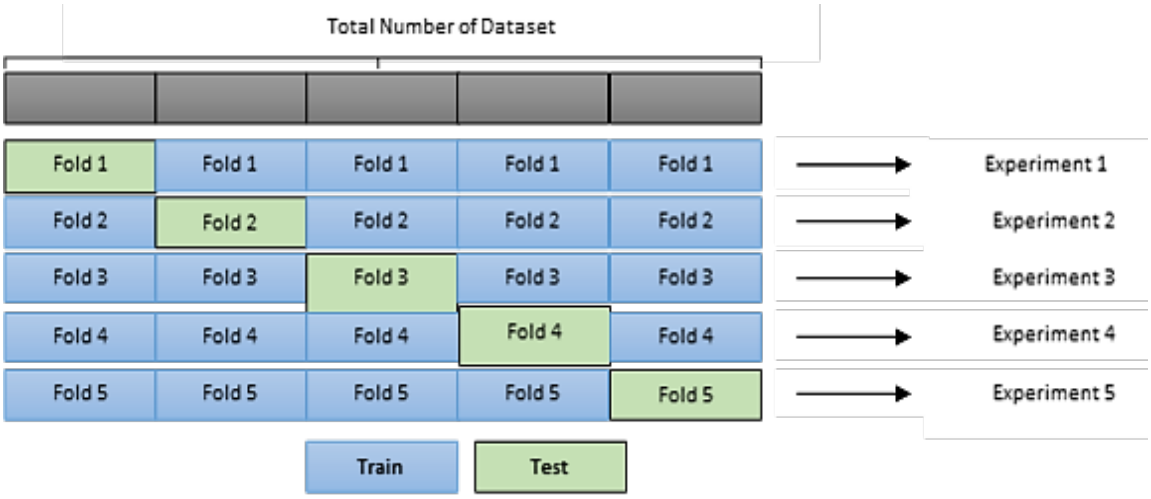

Figure 6: Schematic diagram of the 5-fold cross-validation procedure

4. Results and Evaluation

This section presents all the results based on the processes proposed in our algorithm. We do not focus on pre-processing image methods, calculations, and comparisons; we achieve a straightforward approach process by using linear spatial filtering. To carry out the design model, we use MATLAB R2012b, a high-performance language for technical computing.

4.1 Proposed algorithm results

The KSVM-1 classifier uses 220 MRI images as a dataset. Table 3 explains the number of normal and abnormal images we use for (training and testing). After verifying the proposed model, the model is trained and tested to verify its accuracy. Performance metrics are used to assess the level of performance of the first model (KSVM-1) in classifying a normal brain from an abnormal brain. In the first stage of classification (KSVM-1), we use two kernels. As shown in Figure 7, the best kernel we can consider is a linear function, in terms of accuracy, which increases stably when increasing the training data, unlike the RBF kernel, its accuracy and sensitivity change in descending order with the large increase in the training data. The Linear class satisfies 97.5%, 100%, and 95% in accuracy, sensitivity, and specificity, respectively. The interesting indication in our results besides the accuracy is the sensitivity metric, which is calculated by considering TP and FN terms as explained in Table 1. Thus, a 100% ratio means that all abnormal cases are classified as TP, and FN is equal to zero (no images classified as normal incorrectly). One of the essential objects of this work is to isolate and calculate the tumor area. The use of four clusters based on the K-means technique gives good results in separating the tumor area. We calculate the part of the tumor area through binary coding. The extracted image contains two binary values (1, 0) for the white and black colors, respectively. To calculate the number of white pixels (logic-1) and the brain tumor area, we follow the mouthed described in Section III. Figure 8 shows five samples with their four clusters, tumor segment, and tumor boundary. Table 4 summarizes the calculation of selected samples, and it demonstrates the number of pixels in the tumor segment, tumor area, and tumor boundary. It is essential to extract the texture features from the abnormal images classified by KSVM-1, we use the 2D-DWT technique, which helps to extract and calculate the first-order and second-order features. The extracted features represent the maximum relevant information available to obtain a complete description of the images. Table 5 demonstrates the calculation results of statistical features for five samples. Subsequently, we use the PCA algorithm to reduce the extracted features and increase the processing speed. This technique eliminates unnecessary features and improves the performance of the KSVM-2. We measure several characteristics in the

categorized image area by constructing a structure array whose fields indicate different region features. Then, we return the measurements of the pixel value in a gray-scale image. Accordingly, we accurately identify the affected part. In KSVM-2, a set of MRI images of brains affected by various tumors (both malignant and benign), in the form of "train set. Mat", was used which is a ready-made structure of MRI images that have been carefully selected, and pre-tested. Two classification classes (linear kernel, RBF core) and a set of test images shown in Table 6 were used. The best kernel was a linear function as it achieved 98.57%, 100%.and 97.14% for accuracy, sensitivity, and specificity respectively as shown in the frequency chart in Figure 9. An interesting indicator in our results is the measure of sensitivity; a ratio of 100% means that all cases of malignancy are classified correctly.

Table 3: Data of proposed system / KSVM-1

Total No.of Images		**Training Images**		**Testing Images**	
Normal	Abnormal	Normal	Abnormal	Normal	Abnormal
100	120	80	100	20	20

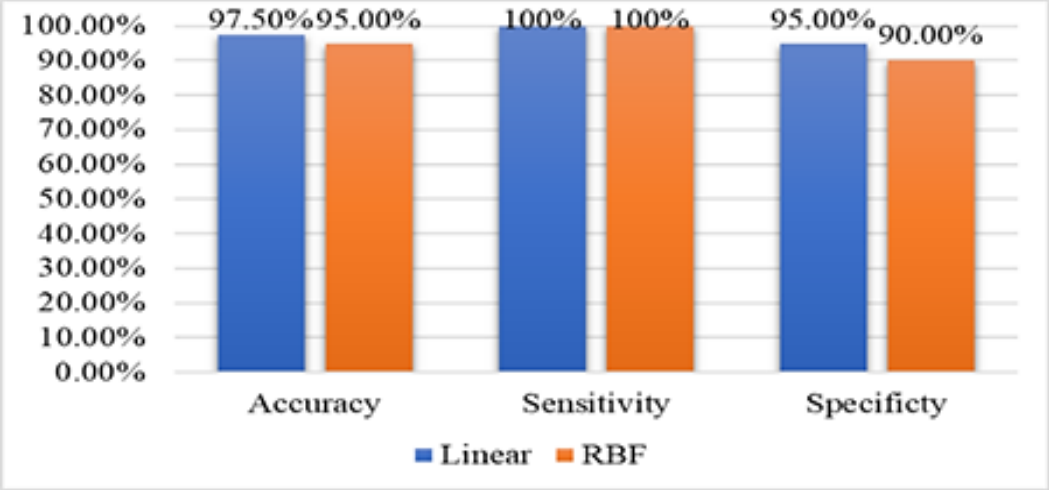

Figure 7: Kernels evaluation metrics of KSVM-1

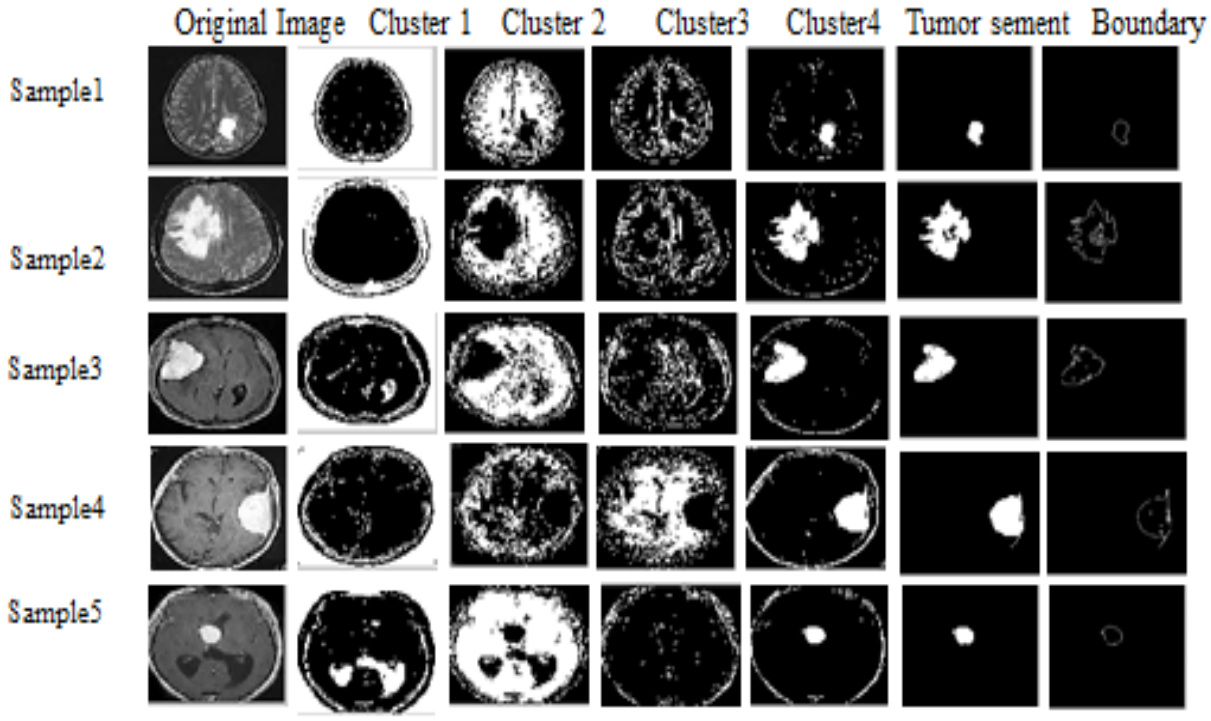

Figure 8: MRI images analysis models into clusters

Table 4: Tumor area calculation

Tumor segment	No. of tumor segment (Pixels) boundary(s)	Tumor area (mm^2)	No. of tumor
Sample 1	606	40.00	90
Sample 2	3665	241.93	622
Sample 3	2337	154.24	300
Sample 4	2022	133.48	540
Sample 5	1589	104.89	323

Table 5: First and second-order features for selected samples

Order	Features	Sample 1	Sample 2	Sample 3	Sample 4	Sample 5
First-order	Mean	0.0026	0.0031	0.0012	0.0030	0.0030
First-order	Standard	0.0898	0.0089	0.0898	0.0898	0.0898
First-order	Skewness	0.7747	0.5114	0.4810	0.7630	0.5139
First-order	Kurtosis	8.7306	7.0859	7.8842	7.0612	5.9389
First-order	Entropy	3.0310	3.3330	3.3649	3.5447	3.4525
Second-	Energy	0.7535	0.7457	0.7702	0.7468	0.7454
Second-	Correlation	0.1422	0.072 6	0.0816	0.0661	0.1365
Second-	Contrast	0.2481	0.2589	0.2386	0.2622	0.2311
Second-	Homogeneit	0.9322	0.9287	0.9354	0.9279	0.9304

Table 6: Data of proposed system / KSVM-2

Total No.	of Images (90)	Training	Images (20)	Testing	Images (70)
Malignant	Benign	Malignant	Benign	Malignant	Benign
45	45	10	10	35	35

Table 7: Setting of 5-fold cross-validation for KSVM-1

Total Number of images (220)		Test images, (44) Images / Fold	
Normal	*Abnormal*	*Normal*	*Abnormal*
100	120	20	24

The K-fold cross-validation assesses our model with an average accuracy, 96.88% and 94.6% for linear kernel and RBF kernel respectively, as shown in Table 8.

Table 8: Cross-validation results

Accuracy % = 100- (Et*100)		Accuracy of linear class		Accuracy of RBF class
Experiment number	*Error rate /exp*	*Accuracy (%)*	*Error rate / exp*	*Accuracy (%)*
1	0.045	95.5%	0.022	97.8%
2	0.022	97.8%	0.045	95.5%
3	0.022	97.8%	0.068	93.2%
4	0.045	95.5%	0.045	95.5%
5	0.022	97.8%	0.090	91.0%
Average	0.0312	96.88%	0.054	94.6%

- Linear kernel , Accuracy = 100- (0.0312*100) = 96.88 %
- RBF kernel, Accuracy = 100- (0.054*100) = 94.6 %

4.2 Cross-Validations Analysis

Cross-validation is necessary for evaluating the designed model. Since the classifier used is trained by a specific set of data, this results in a high classification accuracy of the training data only. Therefore, we need a method to validate the method used. Cross-validation will not increase the final classification accuracy but it does give reliability to the classifier used and can be generalized to other independent data sets. Datasets are randomly divided into separate k-folds of approximately equal size, and each fold is used to test the induced model. The classifier is evaluated by the average accuracy of k. Thus, in our work, a K-fold technique was used to validate KSVM-1. All prediction errors were taken from all K phases and equations (23, 24) were used to calculate the mean cross-validation error rate. For KSVM-1, it uses 5 times of 220 training images. The number of training and

test images per fold for KSVM-1 is tabulated in Table 7. The K-fold cross-validation assesses our model with an average accuracy, 96.88% and 94.6% for linear kernel and RBF kernel respectively, as shown in Table 8.

5. Discussions

We achieve excellent results in all evaluation metrics compared to the results of the previous studies. Some former studies investigate diverse approaches and classifiers to pick the best results. In Table 9, we summarize the best method that has been used to achieve better results. We mark any Not Specified (NS) information, such as the number of images used as a dataset. In addition, we include the unmentioned evaluation metrics of the previous works. The majority of studies do not evaluate their classifiers or algorithms by cross-validation, we used The Cancer Imaging Archive (TCIA) and Kaggle dataset [15, 16], and to validate the proposed algorithm. In our study, we use K-fold cross-validation to evaluate our classifier.

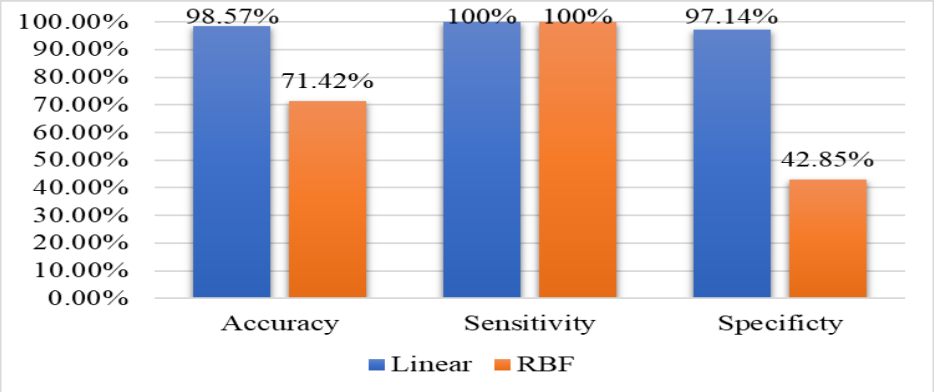

Figure 9: Evaluation metrics of KSVM-2

Table 9: Existing works and the proposed algorithm

Literature	Total Images	Feature extraction	Reduction Technique	Segmentation	Classifier	Normal & abnormal	Benign & Malignant	Cross validation	Evaluation Metrics
[3]	110	**No**	**No**	K-means	SVM	**Yes**	**No**	**No**	Accuracy = 91.49%
[7]	20	GLCM	**No**	K-means& Otsu	SVM	**No**	**Yes**	**No**	Accuracy = 98.51%
[8]	NS	DWT+ GLCM	PCA	Dynamic thresholding	KSVM (RBF)	**No**	**Yes**	**No**	Accuracy = 95.00%
[10]	25	DWT	PCA	**No**	SVM	**Yes**	**No**	**No**	Accuracy = 90.00%
[20]	NS	GLCM	**No**	BWT	KSVM (RBF)	**Yes**	**No**	Bench mark Datas et	Accuracy = 96.51%
[22]	90	DWT	PCA	Threshold-based	KSVM (RBF)	**Yes**	**No**	**No**	Accuracy = 98.00%
[26]	63	DWT	PCA	**No**	SVM	**Yes**	**No**	**No**	Accuracy = 94.86 %
Present Work	90	Pixel values DWT & GLCM	PCA	K-means	KSVM (Linear)	Yes	Yes	K-fold	Accuracy = 98.57% Sensitivity = 100% Specificity = 97.14%

6. Conclusions

This paper proposes a robust model using the most reliable MRI-based techniques to validate abnormal brains. It classifies 220 MRI images by combining two classifiers to improve classification accuracy. The first Kernel Support Vector Machine (KSVM) classifier detects and classifies the abnormal brain exploiting the pixels values as a feature for training and testing. Subsequently, the proposed model uses the abnormal case which is collected as a dataset for the second KSVM classifier. As such, the second classifier detects and classifies abnormal cases to benign and malignant tumors, exploiting the Discrete Wavelet Transform (DWT) technique to extract the global features. Features extraction is followed by the Principal Component Analysis

(PCA) algorithm to reduce features and improve the classifier performance. The evaluation metrics in both classifiers satisfy good accuracy equal to 97.5% and 98.57% in the first and second classifier, respectively, and 100% sensitivity in both. The sensitivity indicates that all abnormal cases are detected correctly, which leads the studies in future work to use this method or similar classifiers to improve other types of disease classifications in high accuracy metrics. This study uses a K-fold cross-validation algorithm to assess the proposed classifier. It achieves accuracy equal to 96.88 % for the first classifier. This study also reinforces the proposed model by assessing the brain segmentation, isolation, and calculation of the tumor area using the K-means method.

Author contribution

All authors contributed equally to this work.

Funding

This research received no specific grant from any funding agency in the public, commercial, or not-for-profit sectors.

Data availability statement

The data that support the findings of this study are available on request from the corresponding author.

Conflicts of interest

The authors declare that there is no conflict of interest.

References

[1] D. N. Louis, the 2016 World Health Organization Classification of Tumors of the Central Nervous System: a summary, Acta. Neuropathol., 131 (2016) 803–820. http://dx.doi.org/10.1007/s00401-016-1545-1

[2] E. A. S. El-Dahshan, H. M. Mohsen, K. Revett, A. B. M. Salem, Computer-aided diagnosis of human brain tumor through MRI: A survey and a new algorithm, Expert. Syst. Appl., 41 (2014) 5526–5545. http://dx.doi.org/10.1016/j.eswa.2014.01.021

[3] G. Singh , M. A. Ansari, Efficient detection of brain tumor from MRIs using K-means segmentation and normalized histogram, India. Int. Conf. Inf. Process., 1 (2017). http://dx.doi.org/10.1109/IICIP.2016.7975365

[4] S. Suhas , C. R. Venugopal, MRI image preprocessing and noise removal technique using linear and nonlinear filters, Int. Conf. Electr. Electron. Commun. Comput. Technol. Optim. Technol., 2017 (2018) 709–712. http://dx.doi.org/10.1109/ICEECCOT.2017.8284595

[5] S. K. Shil, F. P. Polly, M. A. Hossain, M. S. Ifthekhar, M. N. Uddin, An improved brain tumor detection and classification mechanism, Int. Conf. Info. Com. Tec. Conv., (2017) 54–57. http://dx.doi.org/10.1109/ICTC.2017.8190941

[6] Ch. Saha , M. F. Hossain, MRI Brain Tumor Images Classification Using K-Means Clustering, NSCT and SVM, 4th IEEE Uttar Pradesh, Sect. Int. Conf. Electr. Comput. Electron. GLA. Univ. Mathura., (2017) 329–333. http://dx.doi.org/10.1109/UPCON.2017.8251069

[7] G. Birare , V. A. Chakkarwar, Automated Detection of Brain Tumor Cells Using Support Vector Machine, 2018 9th . Int. Conf. Comput. Technol., (2018) 1–4. http://dx.doi.org/10.1109/ICCCNT.2018.8494133

[8] S. C. Kumar , H. D. Phaneendra, Categorization of Brain Tumors using SVM with Hybridized Local-Global Features, Proc. Int. Conf. Comput. Methodol. Commun., (2020) 311–314. http://dx.doi.org/10.1109/ICCMC48092.2020.ICCMC-00058

[9] D. J. Hemanth , J. Anitha, Image pre-processing and feature extraction techniques for magnetic resonance brain image analysis, Commun. Comput. Inf. Sci., 350 (2012) 349–356. http://dx.doi.org/10.1007/978-3-642-35594-3_47

[10] S. Kumar, C. Dabas, S. Godara, Classification of Brain MRI Tumor Images: A Hybrid Approach, Procedia Comput. Sci., 122 (2017) 510–517. http://dx.doi.org/10.1016/j.procs.2017.11.400

[11] J. F. Nunes , P. M. Moreira, Shape based image retrieval and classification, Conf. Info. Syst. Tec., (2010) 1–6.

[12] N. Arunkumar, K-Means clustering and neural network for object detecting and identifying abnormality of brain tumor, Soft Comput., 23 (2019) 9083–9096. http://dx.doi.org/10.1007/s00500-018-3618-7

[13] T. T. Wong, Performance evaluation of classification algorithms by k-fold and leave-one-out cross validation, Pattern. Recognit., 48 (2015) 2839–2846. http://dx.doi.org/10.1016/j.patcog.2015.03.009

[14] Y. Zhang , L. Wu, An MR Brain Images Classifier via Principal Component Analysis and Kernel Support Vector Machine, 130 (2012) 369–388. https://dx.doi.org/10.2528/PIER12061410

[15] The Canser Imaging Archive (TCIA), (2021). https://www.cancerimagingarchive.net Inc., (2019).

[16] S. Abdul Saleem , T. Abdul Razak, Survey on Color Image Enhancement Techniques using Spatial Filtering, Int. J. Comput. Appl., 94 (2014) 39–45. http://dx.doi.org/10.5120/16374-5837

[17] M. A. Nanda, K. B. Seminar, D. Nandika, A. Maddu, A comparison study of kernel functions in the support vector machine and its application for termite detection, Inf., 9 (2018) 5. http://dx.doi.org/10.3390/info9010005

[18] R. Ayachi , N. Ben Amor, Brain tumor segmentation using support vector machines, Lect. Notes. Comput. Sci., 5590 (2009) 736–747. http://dx.doi.org/10.1007/978-3-642-02906-6_63

[19] N. B. Bahadure, A. K. Ray, H. P. Thethi, Image Analysis for MRI Based Brain Tumor Detection and Feature Extraction Using Biologically Inspired BWT and SVM, Int. J. Biomed. Imaging., (2017). http://dx.doi.org/10.1155/2017/9749108

[20] S. H. Wang, Multiple Sclerosis Detection Based on Biorthogonal Wavelet Transform, RBF Kernel Principal Component Analysis, and Logistic Regression, IEEE Access., 4 (2016) 7567–7576. http://dx.doi.org/10.1109/ACCESS.2016.2620996

[21] T. M. Devi, G. Ramani, S. X. Arockiaraj, MR Brain Tumor Classification and Segmentation Via Wavelets, Int. Conf. Wirel. Commun. Signal. Process. Networking., WiSPNET. (2018) 1–4. http://dx.doi.org/10.1109/WiSPNET.2018.8538643

[22] D. Ravichandran, R. Nimmatoori, M. G. Ahamad, Mathematical Representations of 1D, 2D and 3D Wavelet Transform for Image Coding, Int. J. Adv. Comput. Theory. Eng., 5 (2016) 1–8.

[23] N. David , H. Mathieu, Visual quality of printed surfaces: Study of homogeneity, Image Quality and System Performance XI, Proc. SPIE - Int. Soc. Opt. Eng., 9016 (2014) 9016–12. https://doi.org/10.1117/12.2037605

[24] D. Nandi, A. S. Ashour, S. Samanta, S. Chakraborty, Principal component analysis in medical image processing: a study, Int. J. Image. Min., 1 (2015) 45-64. https://doi.org/10.1504/IJIM.2015.070024

[25] K. Nirmalakumari, H. Rajaguru, P. Rajkumar, PCA and DWT Based Gene Selection Technique for Classification of Microarray Data, Proc, Int. Conf. Commun. Electron. Syst., (2018) 850–854. https://doi.org/10.1109/CESYS.2018.8723961